14,04

Differentiation of acoustic emission sources during impact damage of uniaxially loaded quartz ceramics

© I.P. Shcherbakov, A.E. Chmel ¶

Ioffe Institute,
St. Petersburg, Russia

¶ E-mail: chmel@mail.ioffe.ru

Received November 8, 2023
Revised November 8, 2023
Accepted November 10, 2023

Uniaxially compressed quartz ceramic samples were subjected to point impact damage directed orthogonally to the compression. The shock-induced acoustic emission generation was recorded in two frequency ranges: 80−200 kHz and 300−500 kHz. The frequency of the acoustic pulse decreases with increasing size of the emission region, as well as with increasing values of the elastic characteristics of its source. It was found that energy distributions in time sweeps of acoustic emission recorded in the range of 80−200 kHz obey a power law typical for the process of cooperative microcrack formation, whereas distributions in the range of 300−500 kHz are described by an exponential function typical for random, non-interacting sources of acoustic emission such as deformation of ceramic grains. At compression close to the tensile strength limit, the impact caused „pre-threshold" macrofracture of the samples (trigger effect).

Keywords: ceramics, SiO_2, impact fracture, acoustic emission.

DOI: 10.61011/PSS.2024.01.57868.248

1. Introduction

An acoustic emission (AE) method based on the sensitivity to elastic waves that occur in micromechanical acts induced in a solid is widely used to monitor the behavior of various heterogeneous materials subjected to mechanical loading — cement stone [1,2], rock [3,4], ceramics [5,6]. Kersil, commercial quartz ceramics [7] similar in mechanical properties to foreign Corning 7941 was used herein as a model heterogeneous material for the investigation of AE response to impact. A single-component compound is an attractive property of this ceramics for reproducible mechanical tests and is not typical for construction materials and rocks.

Under laboratory conditions, AE generation may be caused by uniaxial [8] or triaxial [4] compression and by impact [9], shear [10] or combined (shear compression) [11] loads applied to the samples. In a present study, a combination of static vertical load and localized orthogonal impact that induced damage on the lateral surface of the sample was used. Such loading geometry simulated real distribution of mechanical forces in building structeres and natural objects whose lower members are compressed vertically and the side surfaces are exposed to propagating seismic waves, tides, volcanic activity and some large-scale engineering procedures.

Apart from sample loading geometry, AE recording frequency range shall be chosen. Acoustic pulse frequency increases with a decrease in the emission area, for example, the microcrack size. Resonance sensors make it possible to detect weaker signals but only in a narrow dimensional range. Wide-band sensors cover actually whole set of formed defects, but their sensitivity is much lower.

In order to differentiate the sources of elastic waves of various scales, data from the wide-band sensor was analyzed in two frequency ranges: 80−200 kHz and 300−500 kHz. Thus, comparison of the energy released during micro damage induced by the local impact was made in spaced AE energy ranges. Statistic analysis of AE time series showed distinction in kind of the emission sources in the specified frequency bands.

2. Samples and equipment

Kersil ceramics is produced by slip forming of fine fused quartz slurry followed by „raw" material (preform) holding at room temperature, drying and calcination. Kersil has a density of 2 g/cm^3, effective porosity of $\sim 10\%$, and OH^--groups content of $\sim 10^3$ ppm.

Photo of the setup for sample loading is shown in Figure 1. Sample surface damage was induced by a pointed striker attached to a pendulum. The shock wave in an uniaxially compressed sample was excited by the orthogonally static load. A support plate was placed behind the sample to avoid its horizontal displacement during impact.

Energy of the striker was constant and equal to 0.12 J. Ultimate (threshold) compression load (without impact load) P_{ul} was preliminary measured. The current load P was varied stepwise from 0 to a critical value at which the sample failure (fragmentation) occurred. After each impact, AE time scans were recorded by a wide-band piezoelectric

Figure 1. General view of the setup for analysis of AE generation in impact damage of the uniaxially compressed sample; detail — compression and impact load center.

transducer made of high-sensitivity PZT ceramics which was attached to the side surface of the sample. Piezoelectric coefficient of the sensor material was two orders of magnitude higher than that of quartz, which minimized the contribution to the effective AE signal in a power law format the test ceramics. AE signals were scanned during 4 ms with time resolution of 40 ns.

3. Results

3.1. Pure impact load

First experiments were conducted without uniaxial static pressure, i. e. using only the striker. The stimulated AE activity from the affected surface area was recorded in 80−200 kHz and 300−500 kHz ranges. Energy yield E during formation of a point defect is proportional to squared amplitude of acoustic pulses: $E \propto A^2$. Figure 2 shows time series of A^2 recorded in the frequency ranges listed above.

Figure 3 shows the energy distributions in AE time series in low-frequency and high-frequency regions. Distributions are shown as $N(E > \varepsilon)$ versus ε with the number of pulses N on the y axis whose energy E exceeds the „threshold“ on the x axis ε that takes the values of pulse energies recorded in the time interval of 0−4 ms after the impact.

The same experimental data are shown in double logarithmic (Figure 3, a) and semilogarithmic (Figure 3, b) scales. It is shown that in double logarithmic coordinates, the distribution $N(E > \varepsilon)$ versus ε of AE data collected in the 80−200 kHz window yields a log-linear dependence

$$\log_{10} N(E > \varepsilon) \propto -b \log_{10}(\varepsilon), \tag{1}$$

where b is the slope of straight line.

Clearing of logarithms, we obtain the distribution $N(E > \varepsilon)$ depending on ε in a power law format

$$N(E > \varepsilon) \propto \varepsilon^{-b}. \tag{1a}$$

Power function is the only solution of the self-similarity equation

$$N(\lambda E) = \lambda^{-b} N(E), \tag{2}$$

where λ is the scale factor. Scale invariance of the micro defect accumulation process occurs as a result of

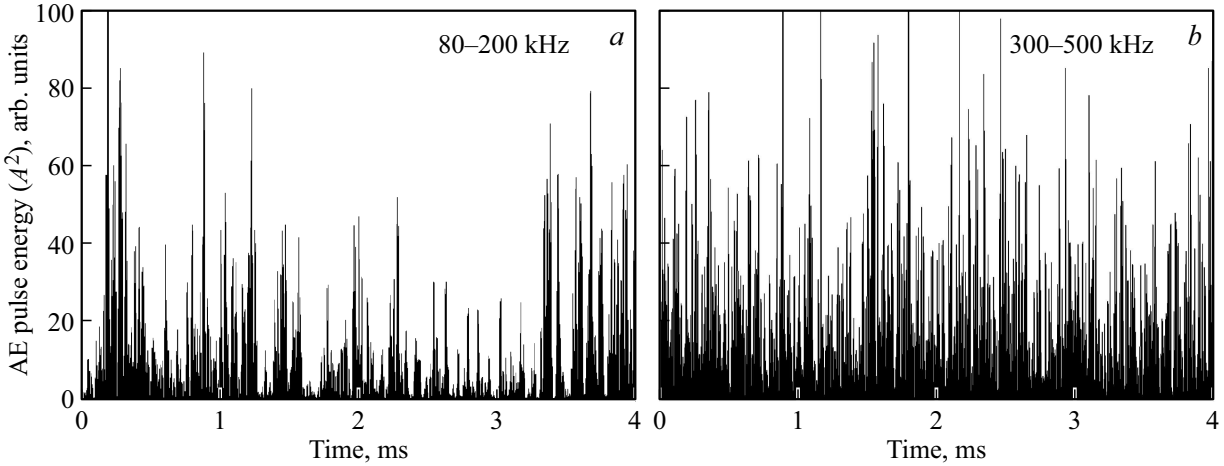

Figure 2. AE amplitude time scans in 80−200 kHz (a) and 300−500 kHz (b) ranges recorded after impact exposure of the sample free of static load.

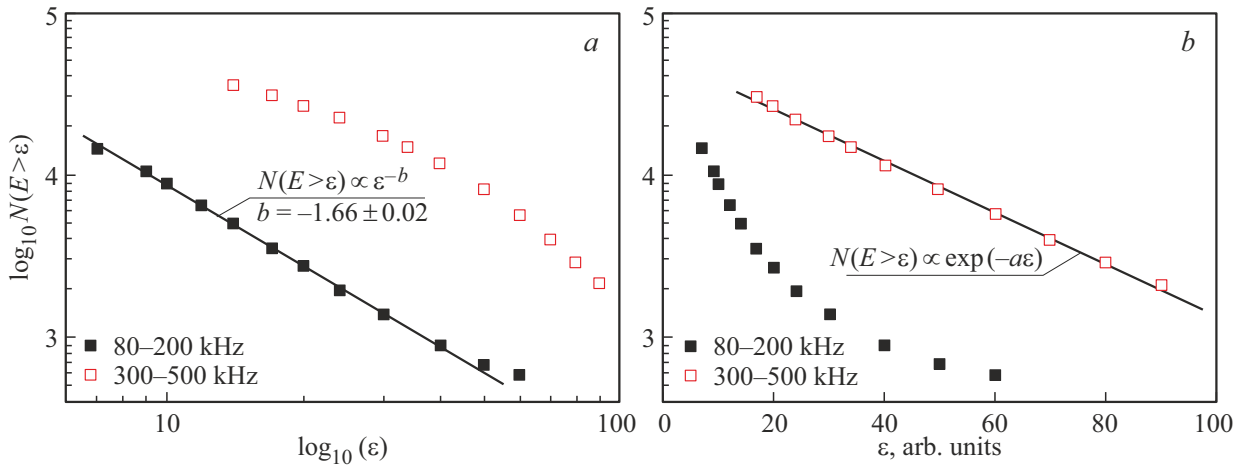

Figure 3. Energy distributions in AE time series in frequency ranges of 80−200 kHz and 300−500 kHz after impact exposure of the sample free of static load in double logarithmic (*a*) and semilogarithmic (*b*) scales.

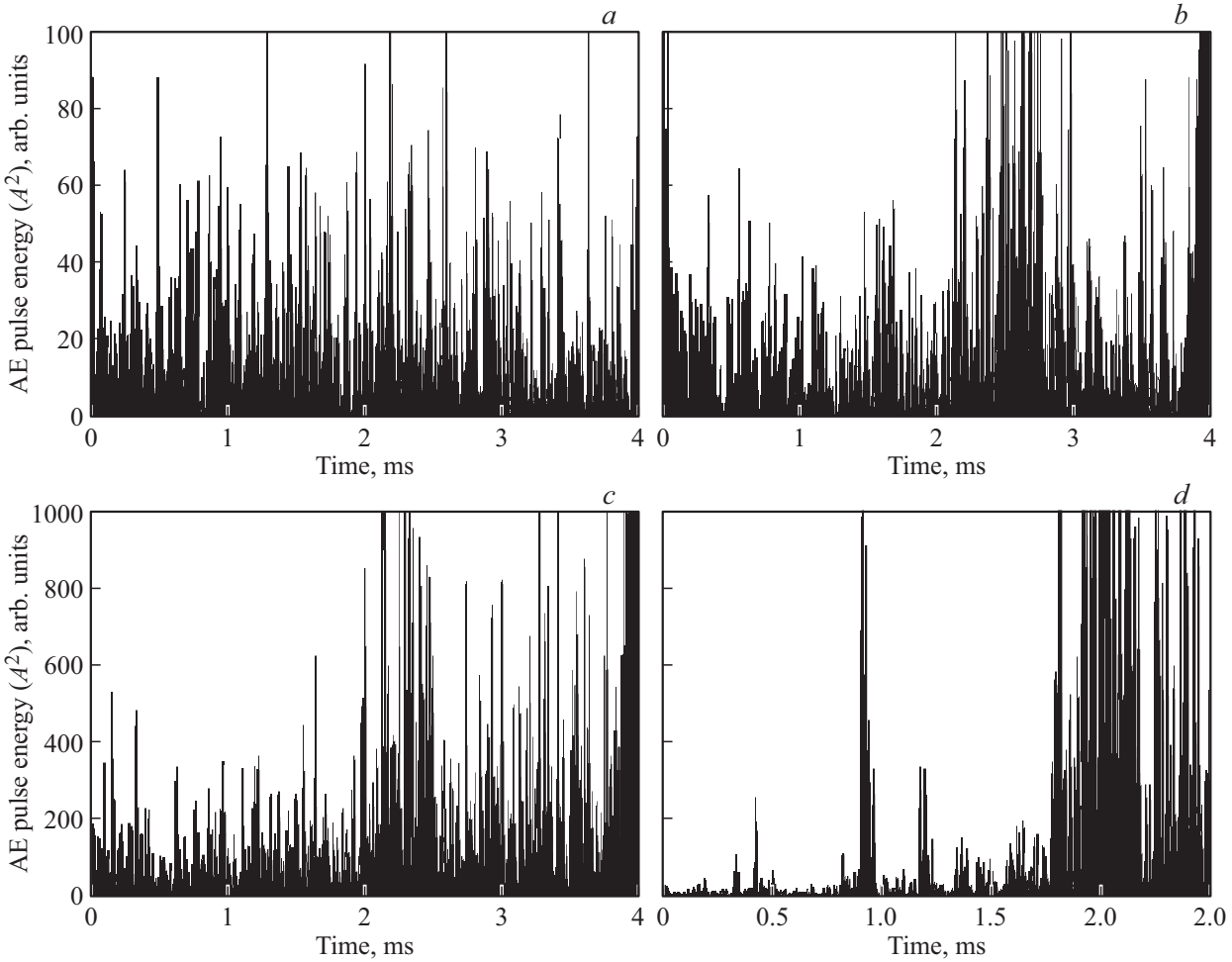

Figure 4. Impact-induced AE time scans within 80−200 kHz at compressions $0.3P_{ul}$ (*a*); $0.6P_{ul}$ (*b*), $0.9P_{ul}$ (*c*) and $0.93P_{ul}$ (*d*).

„long-range“ interactions between individual local failure events that interact with each other at distances exceeding the geometrical dimension of the affected domain in the material [12].

Energy distribution in window 300−500 kHz did not show log-linear dependence (1). However, in semilogarithmic coordinates (Figure 3, *b*), experimental points are applied to the line with slop *a* in accordance with the

following relation

$$\log_{10} N(E > \varepsilon) \propto -a\varepsilon, \tag{3}$$

that may be written exponentially

$$N(E > \varepsilon) \propto e^{-a\varepsilon}. \tag{3a}$$

Poissonian type distribution function is a typical feature of random events that do not interact with each other.

3.2. Samples under static pressure

For experiments with impact damage of ceramics exposed to orthogonally applied static compression, the samples were placed into the hydraulic press which imposed sequential loads with relative pressures P/P_{ul} 0.3, 0.6, 0.9, at which the striker impact did not caused global failure. However, the impact at the static pressure within $0.9P_{ul} < P < P_{ul}$ caused global failure of the sample which may be defined as „subthreshold" failure. Figure 4 shows time scans of generated AE pulses in the low-frequency window 80–200 kHz, including a shortened scan (Figure 4, *d*) that was recorded during impact failure of the sample under load $P = 0.93P_{ul}$.

Figure 5 shows energy distribution in the AE pulse series. Slope of lines *b* tends to decrease with an increase in static load. It is conspicuous a very low slope of the plot for „subthreshold" failure ($P = 0.93P_{ul}$) compared with those at static load range from zero to $P = 0.9P_{ul}$. The slope of dependence (1) reflects a relative contribution of low-energy and high-energy pulses to AE [13]: the lower the slope the more number of larger damages is imposed by the striker impact.

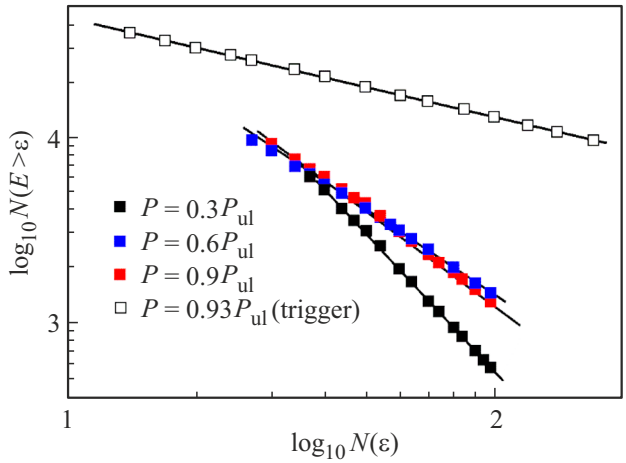

Figure 5. Energy distributions in AE pulse series at compression pressures from $P = 0.3P_{ul}$ to $P = 0.93P_{ul}$.

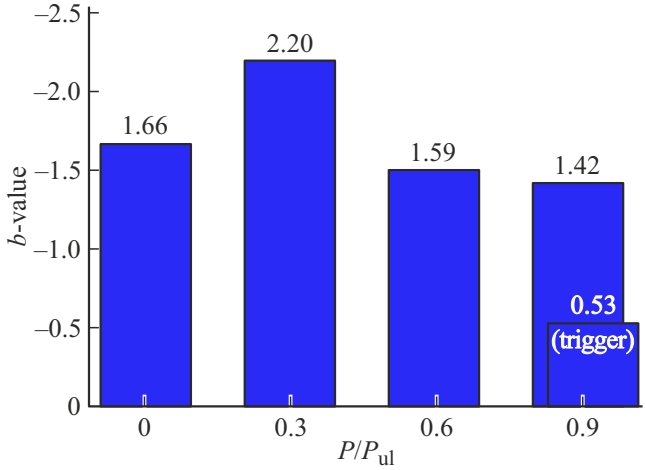

Figure 6. Bar diagram of *b* variation depending on the degree of static compression of the sample.

4. Discussion

AE activity excited by the point impact was observed at static uniaxial compression from zero to a value approaching the failure threshold (but still subcritical). The wide-band AE signal receiver made it possible to distinguish two different emission sources in 80–200 kHz and 300–500 kHz ranges. The power law energy distribution as observed in the low-frequency window is typical for cooperative accumulation of damages thanks to interaction between the generated microcracks. The AE pulse frequency is inversely proportional to the damage size. Therefore, the acoustic generation in the high-frequency window is caused by formation of more confined defects — such as local plastic deformation of ligaments between pores and/or pore displacement with acoustic wave emission. Random energy distribution of pulses recorded in window 300–500 kHz has shown that pulse sources belong to micromechanical phenomena that do not affect each other due to insufficient interaction energy at a distance.

Accumulation of microcracks in the range of 80–200 kH is characterized by the *b*-value in equation (1) that was first introduced in the Gutenberg–Richter law. Variation of this parameter in various static loading conditions is shown in the bar diagram (Figure 6). It can be seen that the minimum compression of the sample up to $0.3P/P_{ul}$ resulted in significant increase in the *b*-value, that, as described above, is indicative of a decrease in the contribution of larger AE acts to energy distribution. This may be explained by primary increase in the material density. With an increase in compression load up to $0.6\,P/P_{ul}$ and then to $0.9\,P/P_{ul}$, the *b*-value has decreased again, reflecting the relative increase in the energy of new microcracks. In the load range of $0.9 < P/P_{ul} < P_{ul}$, a trigger effect occurred — „subthreshold" global material failure (fragmentation). In the latter case, the *b*-value was several times lower, as is to be expected when large cracks are formed. This result coincides with data in [3], where it was pointed out that when the trigger effect occurred in granite, the *b*-value was lower than in common failure under the threshold load.

5. Conclusion

AE signal generation during impact damage of laboratory quartz ceramics samples exposed to compression pressure was recorded in 80−200 kHz and 300−500 kHz ranges. Comparative statistical analysis of energy distribution in AE scans has shown the difference of the material structure failure processes reflected in the specified AE frequency ranges. In a lower-frequency range, energy distribution in AE pulses followed the power law specific for scale-invariant accumulation of microcracks, while the emission in a higher-frequency region zone was described by the exponential function typical for random statistical processes. In this case, such processes may include deformation displacements in ligaments between pores which (as opposed to cracks) do not show any interaction between each other due to insufficient energy of such structural changes.

Plotted pulse energy distributions constructed in the low-frequency range were characterized by the *b*-value widely used in seismology to assess the number of events with different energy yield. Static loading caused an increase in relative contribution of fine microcracks, but in case of trigger fracture, sharp increase in the proportion of damage acts with high energy yield was observed.

Conflict of interest

The authors declare that they have no conflict of interest.

References

[1] D.G. Aggelis. Mech. Res. Commun. **38**, 153 (2013).
[2] D.D. Mandal, M. Bentahar, A. El Mahi, A. Brouste, R. El Guerjouma, S. Montresor, F.B. Cartiaux. Materials **15**, 3486 (2022).
[3] J. Davidsen, T. Goebel, G. Kwiatek, S. Stanchits, J. Baró, G.J. Dresen. J. Geophys. Res. Solid Earth **126**, e2021JB022539 (2021).
[4] B. Haimson, C. Chang. Int. J. Rock. Mech. Min. Sci. **37**, 285 (2000).
[5] J. Aué, J.T.M.D. Hosson. J. Mater. Sci. **33**, 5455 (1998).
[6] G. Ojard, M. Mordasky, R. Kumar. AIP Conf. Proc. **1949**, 230028 (2018).
[7] V.V. Vikulin, I.L. Shkarlupa, S.M. Itkin, F.Ya. Borodai. Patent RF RU2385850 (2008). (in Russian).
[8] C.H. Sondergeld, L.H. Estey. Geophys. Res. Solid Earth **86**, 2915 (1981).
[9] X. Liu, M. Pan, X. Li, J. Wang. Advances in Acoustic Emission Technology: Proceedings of the World Conference on Acoustic Emission — 2015. Springer Proceedings in Physics **179**, 135 (2015).
[10] X. Lei. Appl. Sci. **9**, 2498 (2019).
[11] Y. Cao, J. Xu, L. Chen, P. Wu, F. Shaikh. Sci. Rep. **10**, 22051 (2020).
[12] D.D. Bowman, G. Ouillon, C.G. Sammis, A. Sornette, D. Sornette. J. Geophys. Res. **103**, 24359 (1998).
[13] P. Li, M. Cai, Q. Guo, F. Ren. Lithosphere, *Special* **11**, 3594940 (2022).

Translated by E.Ilinskaya